Research article

Journal of MASS SPECTROMETRY

Received: 23 January 2016 Revised: 4 March 2016 Accepted: 14 March 2016 Published online in Wiley Online Library

(wileyonlinelibrary.com) DOI 10.1002/jms.3762

Mapping *Dicorynia guianensis* Amsh. wood constituents by submicron resolution cluster-TOF-SIMS imaging

Quentin P. Vanbellingen,[a†] Tingting Fu,[a,b] Claudia Bich,[a] Nadine Amusant,[c] Didier Stien,[a,d] Serge Della-Negra,[b] David Touboul[a] and Alain Brunelle[a]*

The preparation of tropical wood surface sections for time-of-flight secondary ion mass spectrometry imaging is described, and the use of delayed extraction of secondary ions and its interest for the analysis of vegetal surface are shown. The method has been applied to the study by time-of-flight secondary ion mass spectrometry imaging with a resolution of less than one micron of a tropical wood species, *Dicorynia guianensis*, which is one of the most exploited wood in French Guiana for its durable heartwood. The heartwood of this species exhibits an economical importance, but its production is not controlled in forestry. Results show an increase of tryptamine from the transition zone and a concomitant decrease of inorganic ions and starch fragment ions. These experiments lead to a better understanding of the heartwood formation and the origin of the natural durability of *D. guianensis*.

Keywords: TOF-SIMS; mass spectrometry imaging; tropical wood; *Dicorynia guianensis*; tryptamine; heartwood formation

Introduction

Time-of-flight secondary ion mass spectrometry (TOF-SIMS) imaging is a powerful tool to study the spatial distributions of natural products on a surface. Although the first biological applications of this technique were in mammalian tissue sections and single cell imaging,[1,2] this tool has also been utilized several times to study samples from *Plantae* kingdom such as seeds,[3–5] leaf cuticles,[6] and microalgae.[7,8] The first report of wood analysis appeared in 2005 with the study of spatial distribution of a diterpene phenol called ferruginol in the sapwood and the heartwood of the Japanese cedar *Cryptomeria japonica*. In this study, ferruginol has been detected homogenously in the heartwood.[9] In 2007, Tokareva *et al*. studied how to prepare wood sample for TOF-SIMS imaging, in order to investigate the composition of lignin and inorganic species on sections of Norway spruce (*Picea abies* Karst.).[10] A new sample preparation method has been proposed consisting in the use of organic solvents in order to decrease the matrix effects induced by wood extractives. The spatial distribution of hinokinine between the sapwood and the heartwood of Japanese cypress (*Chamaecyparis obtuse*) has been also studied by TOF-SIMS for dendrochronology on a cultural heritage sample.[11] It has been shown that hinokinine is exclusively localized in the ray parenchyma cells and is more abundant in the transition zone, which corresponds to the area between sapwood and heartwood and where the parenchyma cells undergo apoptosis. Moreover, the same group studied the difference of lignin and inorganic compositions between sapwood and heartwood. While a homogeneous composition of lignin was found in the two types of wood tissue, changes in sodium, magnesium and calcium concentrations were measured between sapwood, heartwood and in the transition zone.[12] In 2011, Goacher *et al*. published an article about statistical analysis of ion species detected from wood samples, leading to a list of characteristic fragment ions of polysaccharide and lignin.[13] The spatial distribution of G-lignin and S-lignin around parenchyma cells of poplar (*Populus trichocarpa*) was also described. After removing by sputtering with a C_{60} ion beam the damages made during the sample preparation of the transversal wood section, an enrichment in G-lignin was observed in the middle lamella.[14] The first three-dimensional imaging analysis of wood cells was provided by Jung *et al*. in 2012, using the dual-beam depth profiling method.[15] This method has been applied to a transversal section of poplar (*Populus tremula x alba*) to study the cellulose enrichment in different cellular layers of tension wood.[16] In 2013, Kuroda *et al*. coupled a cryo-TOF-SIMS/SEM system for accurate spatial distribution of chemical compounds on a transversal section of Japanese cedar. This cryo-

* *Correspondence to: A. Brunelle, Institut de Chimie des Substances Naturelles, CNRS UPR 2301, Université Paris-Sud, Université Paris-Saclay, Avenue de la Terrasse 91198 Gif-sur-Yvette, France. E-mail: Alain.Brunelle@cnrs.fr*

a *Institut de Chimie des Substances Naturelles, CNRS UPR 2301, Univ. Paris-Sud, Université Paris-Saclay, Avenue de la Terrasse, 91198 Gif-sur-Yvette, France*

b *Institut de Physique Nucléaire, UMR8608, IN2P3-CNRS, Université Paris-Sud, 91406 Orsay, France*

c *CIRAD, UMR EcoFoG, CNRS, AgroParisTech, INRA, Université des Antilles, Université de Guyane, 97310 Kourou, France*

d *Sorbonne Universités, UPMC Université Paris 06, CNRS, Laboratoire de Biodiversité et Biotechnologies Microbiennes (LBBM), Observatoire Océanologique, 66650 Banyuls-sur-mer, France*

† *Current address: Department of Chemistry and Biochemistry, Florida International University, Miami, FL, USA*

Journal of MASS SPECTROMETRY

technique allows the detection of water, inorganics and metabolites at the same time.[17] In 2014, Saito *et al.* studied the immobilization of aluminum in the cell wall of maple (*Acer micranthum*),[18] and Gerber *et al.* developed a method to determine the wood cell wall thickness by TOF-SIMS.[19] This non-exhaustive state-of-the-art of wood analysis by TOF-SIMS shows that this mass spectrometry imaging method allows studying both inorganics and organics in different kinds of wood species.

Table 1 shows the sample preparation methods used for different wood species and their respective Janka hardness. Three main methods have been used. To study inorganics, metabolites and structural polymers, sliding microtomes have been used, while to focus on structural materials, it is necessary to remove the metabolites, which may induce matrix effects. This is why Tokareva *et al.* used Soxhlet washing.

High density tropical wood TOF-SIMS analysis has never been described in the literature. An obvious reason could be that hard tropical wood species are very difficult to cut in transversal orientation (Janka hardness of *D. guianensis* is 1720 lbf, Table 1). In French Guiana, *D. guianensis* is one of the most exploited Amazonian wood species, with 20 000 m^3 of logs felled each year. This species is much appreciated for its hard, durable, dark brown heartwood.[20] *D. guianensis* heartwood is resistant against wood pests such as xylophagous insects, marine borers and fungi. Because of its economic importance, its chemical composition has been studied recently.[21] The aim of the present work is to focus on changes of chemical composition, which occur around the transition zone to obtain a better understanding of heartwood formation and durability. For this purpose, it is necessary to study the chemical distribution on a large area between sapwood and heartwood and at a subcellular level. Therefore, the sample preparation method to obtain a flat and undamaged transversal wood surface is also discussed leading to acquisition of high spatial and high mass resolution images with a delayed extraction (DE) of secondary ions, as previously described by Vanbellingen *et al.*[22]

Material and methods

D. guianensis Amsh. wood sample

The samples were taken from a *D. guianensis* Amsh. adult tree (diameter 30 cm and height 27 m) harvested from the Paracou forest in French Guiana (5°15′N and 52°55′W). The tree was chosen as representative of the species (adult, without damage and with an intact crown), according to the method used by Rutishauser *et al.*[23] This method is based on analysis of the crown structure and of its fragmentation degree to evaluate the development of the tree (juvenile or adult specimens, possible damage like headless trunk, senescent tree or intact crown).

Sample preparation

Radial and wet microtome transverse sections

Radial sections of *D. guianensis* were prepared directly from a block (length ~10, width ~6, and thickness ~10 mm) of wood. In order to soften the wood for transverse sections, a small block (~1 cm × 1 cm × 1 cm) was put in a 100 ml beaker, which contained 50 ml ultrapure water. After 4 h, the wood block was air dried for 1 h. Then, 16 μm thick transverse sections were prepared using a microtome. In both cases, sections of 16 μm thickness were cut at room temperature and deposited on a stainless steel plate with the help of double-sided conductive adhesive tape (3M Core Series 2-0300). Optical images of the wood sections were obtained with the use of an Olympus BX51 microscope (Olympus France, Rungis, France), equipped with 1.25× to 50× lenses, a motorized scanning stage (Marzhauser Wetzlar GmbH, Wetzlar, Germany), a SC30 color camera, and monitored by the Olympus Stream Motion (Olympus France, Rungis, France) 1.9 software.

Dry ultramicrotome sections/surfaces

Wood blocks of 1 cm × 1 cm × 1 cm taken from the sapwood, the transition zone and the heartwood have first been cut into the shape of pyramid. The top of the pyramid presents the transverse orientation. The resulting blocks were then sectioned using an EM UC6 Ultramicrotome (Leica Microsystèmes, SAS, Nanterre, France) equipped with a DIATOME Cryotrim 45° diamond knife (Leica Microsystèmes, SAS). Surfaces were cut at a speed of 2 mm·min^{-1}, at 500 and 200 nm thicknesses. In the following, the analyzed samples will be named as being sections, although the analyses are made at the surface of the small wood blocks.

Analysis of standards

A volume of 1 μl of pure tryptamine (Sigma-Aldrich, St-Quentin-Fallavier, France) solution at 1 mg·ml^{-1} was deposited on a gold plate. Analyses were performed with a primary ion dose of 8.9×10^{10} ions·cm^{-2}.

Tuning of the mass spectrometer

Experiments were performed using a commercial TOF-SIMS IV (ION-TOF GmbH, Münster, Germany), located at the Institut de Chimie des Substances Naturelles (CNRS, Gif-sur-Yvette, France). This instrument is equipped with a liquid metal ion gun (LMIG), which

Table 1. Janka hardness and related sample preparation used for TOF-SIMS imaging for different wood species

Wood species	Janka hardness (lbf)	Sample preparation	Ref
Cryptomeria japonica	320	Sliding microtome	9,17
Picea abies Karst.	380	Cryomicrotome + soxhlet extracted	10
Chamaecyparis obtuse	unknown	Sliding microtome	11,12
Pinus contorta Dougl.	480	Soxhlet extracted + ultramicrotome	13
Populus trichocarpa	350	Wax embedding (formaldehyde – acetic acid – ethanol) + microtome	14
Populus tremula x alba	410	Cryomicrotome + soxhlet extracted	15
Acer micranthum	unknown	Sliding microtome	18
Dicorynia guianensis	1720	Ultramicrotome	This article

Data provided from the wood database (http://www.wood-database.com; 1 lbf equals 4.45 N)

delivers a pulsed Bi_n^{q+} (with n = 1–7 and q = 1 or 2) ion beam. Primary ions impact the sample surface with a kinetic energy of 25 qkeV at an incidence angle of 45°. All the experiments presented were carried out with Bi_3^+. The emitted secondary ions were accelerated to a kinetic energy of 2 keV (2 kV extraction) toward a field-free region and a single stage reflectron (first-order compensation). Secondary ions were post-accelerated to a kinetic energy of 10 keV before hitting the detector composed of a micro-channel plate, a scintillator and a photomultiplier. Between two successive primary ion pulses, a low energy (~20 eV) electron flood gun was used to neutralize the sample surface. Pulsed primary ion currents were measured with a Faraday cup located on the grounded sample holder. Two ion beam focusing modes have already been described in detail in the literature.[24–26] The so-called high current bunched (HCBU) mode consists of using three electrostatic lenses and a primary ion buncher system, thus enabling very short pulses of less than one nanosecond. In this case, high mass resolution is achieved. The drawback is a larger beam diameter resulting in moderate spatial resolution around a few microns. The so-called burst alignment (BA) is a mode, which allows for a very narrow beam diameter, well below one micron (~400 nm), using a pair of electrostatic lenses. The disadvantage of this method is the time width of the primary ion pulses, several tens of nanoseconds on the sample plane, which typically results in unit mass resolution. Another disadvantage is the low current of primary ions that necessitates long analysis times. Then another setting mode was used, which adds to the BA focusing mode a delayed extraction (DE) for the secondary ions, as previously described in detail.[22] In this mode, called burst alignment plus delayed extraction (BA + DE), the primary ion pulse duration was fixed to 100 ns and an ion current of 0.07 pA was measured by the Faraday cup. The DE time was fixed at 1235 ns. It has to be noticed that this value is in fact the sum of several internal delays of the electronics and of the true delay of extraction, which is in fact about 100 ns. This mode enables to acquire images with both high mass and spatial resolutions. The mass resolution is even better than in the HCBU mode because the DE compensates for small height differences at the surface of the sample. Mass resolution values measured in BA + DE are typically 8000 ($M/\Delta M$, FHWM, for ions at *m/z* 385) instead of ~3000 in the HCBU mode.[22]

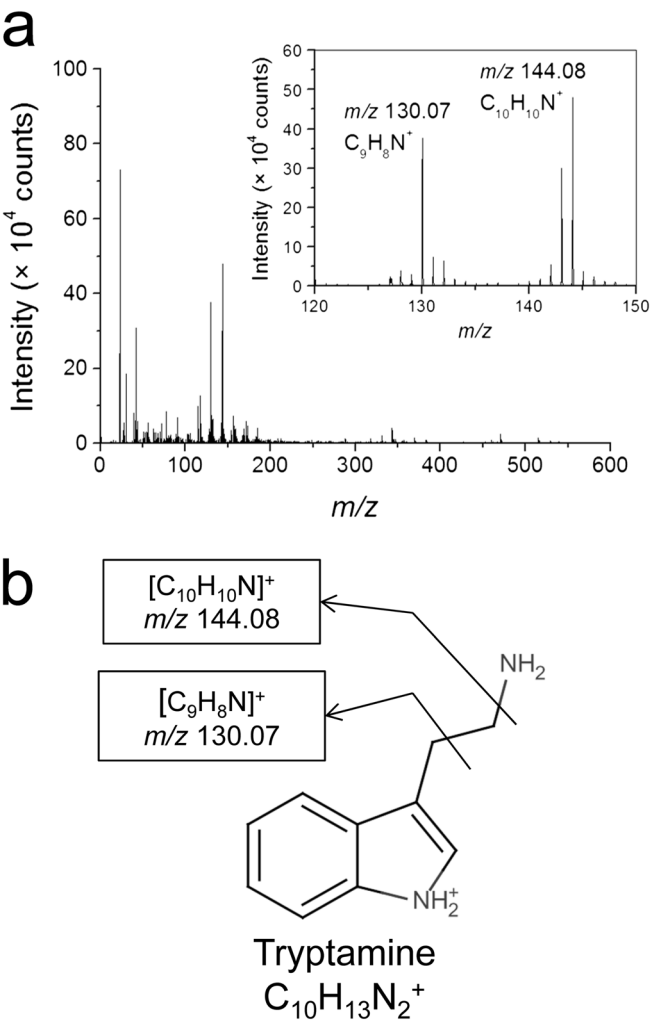

Figure 1. TOF-SIMS analysis of pure standard of tryptamine. (a) Positive ion mass spectrum; (b) Fragmentation pattern.

Large area imaging

At the surface of the radial wood section, a large area of 8000 μm × 2000 μm was analyzed using the HCBU mode. The number of pixels was fixed to 1024 × 256, resulting in a pixel size of 7.8 μm. The images were recorded with a fluence of 1.1×10^{10} ions · cm^{-2}. In this setting mode, because of the low initial kinetic energy distribution of the secondary ions, the relationship between the time-of-flight and the root square of the *m/z* value is always linear over the mass range. The mass calibration was always internal, and the peaks used for the initial calibration were H^+, H_2^+, H_3^+, C^+, CH^+, CH_2^+, $C_2H_3^+$ and $C_2H_5^+$ for the positive ion mode and C^-, CH^-, CH_2^-, C_2^-, C_3^- and C_4H^- for the negative ion mode.

High spatial and mass resolution imaging

At the surface of the wood block, areas of 400 μm × 400 μm were analyzed with a pixel size of 400 nm. The images were recorded with a fluence of 4.0×10^{12} ions · cm^{-2}. Using a single stage DE, the lighter ions, below *m/z* 20, have a larger energy deficit due to their position when the extraction potential is applied and cannot be collected on the detector. Another consequence of the DE is that the relationship between the time-of-flight and the root square of the *m/z* value is not linear over the whole mass range. The ions $C_7H_7^+$ (*m/z* 91.05), $C_7H_9^+$ (*m/z* 93.07), $C_7H_{11}^+$ (*m/z* 95.09), $C_8H_9^+$ (*m/z* 105.07) and $C_{11}H_9O_3^+$ (*m/z* 189.06) have been chosen to achieve the mass calibration in positive ion mode, while C_3^- (*m/z* 36.00), C_4H^- (*m/z* 49.01), $C_2H_3O_2^-$ (*m/z* 59.01) and $C_3H_3O_2^-$ (*m/z* 71.01) ions were used for negative ion mode, but the mass calibration needed to be refined in some cases to ensure a good precision of the mass assignments.

The acquisition in the BA + DE mode requires more than 1 h. During the acquisition, it is possible that some scans are shifted, thus making the image blurred. To improve the quality of the image, the data acquisition and processing software SURFACE LAB 6.5 (ION-TOF GmbH, Münster, Germany), which was used for all the acquisitions, allows calculating the shift and correcting it.

For all ion images recorded, the name of the compounds or the *m/z* value of the peak centroid, the maximal number of counts (MC) in a pixel, and the total number of counts are written below each image. The color scales correspond to the interval [0, MC].

Results and discussion

Analysis of standard

Tryptamine and other indole alkaloids were already isolated from *D. guianensis*.[27] A pure standard of tryptamine was analyzed to help

Journal of MASS SPECTROMETRY

and reinforce the mass assignments. Figure 1(a) shows the TOF-SIMS positive ion mass spectrum of tryptamine. Two main fragments have been detected corresponding to $[C_9H_8N]^+$ at *m/z* 130.07 and $[C_{10}H_{10}N]^+$ at *m/z* 144.08. The molecular ion of tryptamine has not been detected. The fragmentation pattern of tryptamine in TOF-SIMS is described in Fig. 1(b).

Comparison between the different sample preparation methods

Because wood is a three-dimensional structured anisotropic material, the mechanical resistances met by the blade are different depending on the cutting orientation. To obtain a tangential or radial section, the fiber cells are parallel to the stainless microtome blade. In this direction, the blade does not meet any strong mechanical resistance. It is then possible to obtain a large size section in radial orientation of the wood sample. Figure 2(a) shows an optical image of a radial section of *D. guianensis*. The quality of such a radial section is not sufficient to distinguish the different kinds of cells, which compose the wood, but yet allows studying the sapwood/heartwood boundary (white vertical dotted lines in Fig. 2(a)). To obtain a transversal section, the blade was oriented perpendicular to the vessels and fiber cells. In this case, the blade meets a greater mechanical resistance and for some hardwood species, it is impossible to cut it without damaging the vegetal tissue, or even the blade. This is the case for *D. guianensis,* which exhibits a Janka hardness of 1720 lbf. To make the sample softer, a wood block was placed in water before being cut by the microtome blade, as described previously. Figure 2(b) shows the optical image of the obtained transversal section of *D. guianensis*. The quality of the section is sufficient to distinguish all the different kinds of cells. Finally, another sample preparation was investigated to obtain transverse sections, using an ultramicrotome with a diamond knife. This method is usually employed to obtain very thin sections of a few hundreds of nanometers only and is very similar to the one, which has already been used to prepare samples from cultural heritage artifacts.[28,29] Because the sections are very thin and difficult to handle, the block has been directly analyzed after being cut by the diamond blade; the ultramicrotome is used more as a 'polishing' device rather than as a cutting one. Figure 2(c) shows an optical image of the surface thus prepared. Herein, the high quality of the surface allows distinguishing the different kinds of cells, which compose the wood material. An advantage of this last method is that the sample is never wet, thus preserving it from any risk of compound delocalization.

Figure 3 shows images of Ca^+ and $CaOH^+$ ions recorded from the surface of a wet sample cut with a microtome [Fig. 3 (a)] and from the surface of a dry sample cut with an ultramicrotome and a diamond blade [Fig. 3(b)], respectively. In Fig. 3 (a) these ions are randomly distributed with small dots and aggregates without spatial correlation with the tissue histology, while in Fig. 3(b) the calcium ions are always detected in the cell walls. This shows that wetting the sample with water can delocalize some ion species. The drawback of the dry method is the size of the sample, which is limited to less than 1 mm by the width of the diamond knife. However, this method allows to obtain a plane and clean surface, without noticeable delocalization.

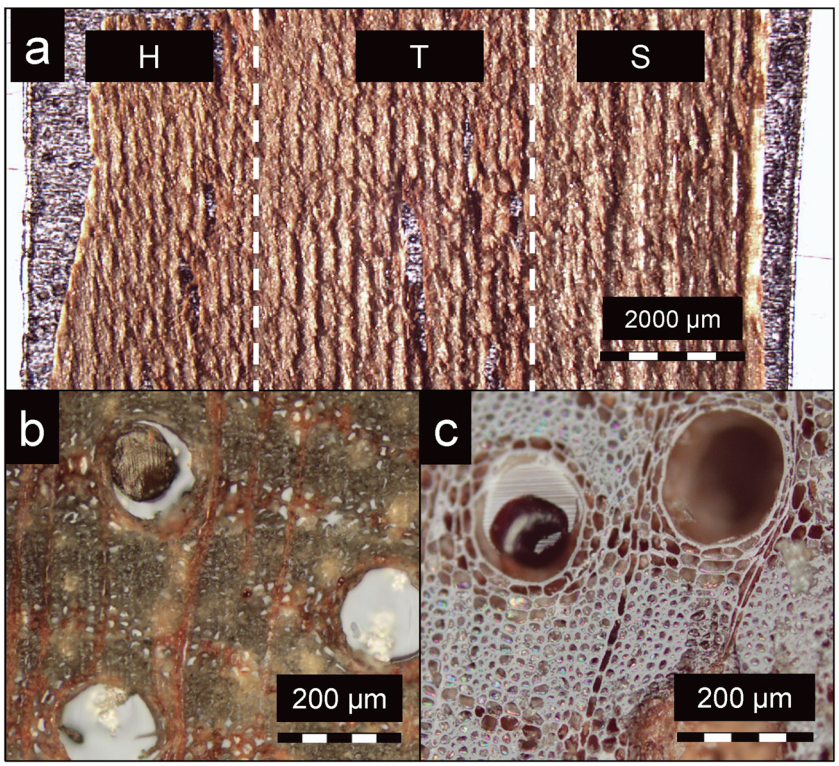

Figure 2. Optical images of samples obtained with different preparation methods. (a) radial section with a microtome. The two vertical white dotted lines indicate the limits between heartwood (H), transition zone (T) and sapwood (S). Scale bar 2000 µm (b) Transversal section of a wet sample (heartwood) made with a microtome. Scale bar 200 µm (c) Transversal section of a dry sample (heartwood) made with an ultramicrotome equipped with a diamond blade. Scale bar 200 µm.

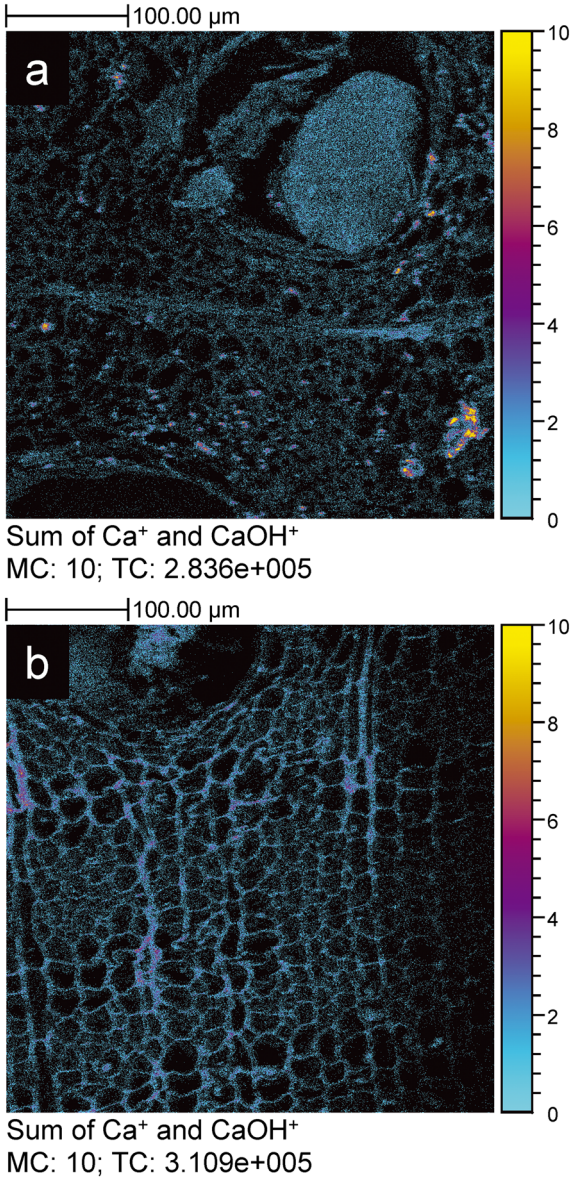

Figure 3. Ion images of the sum of Ca^+ and $CaOH^+$ ions at the surface of a transverse section (heartwood) obtained with (a) a wet sample cut with a microtome, (b) a dry sample cut with an ultramicrotome equipped with a diamond blade.

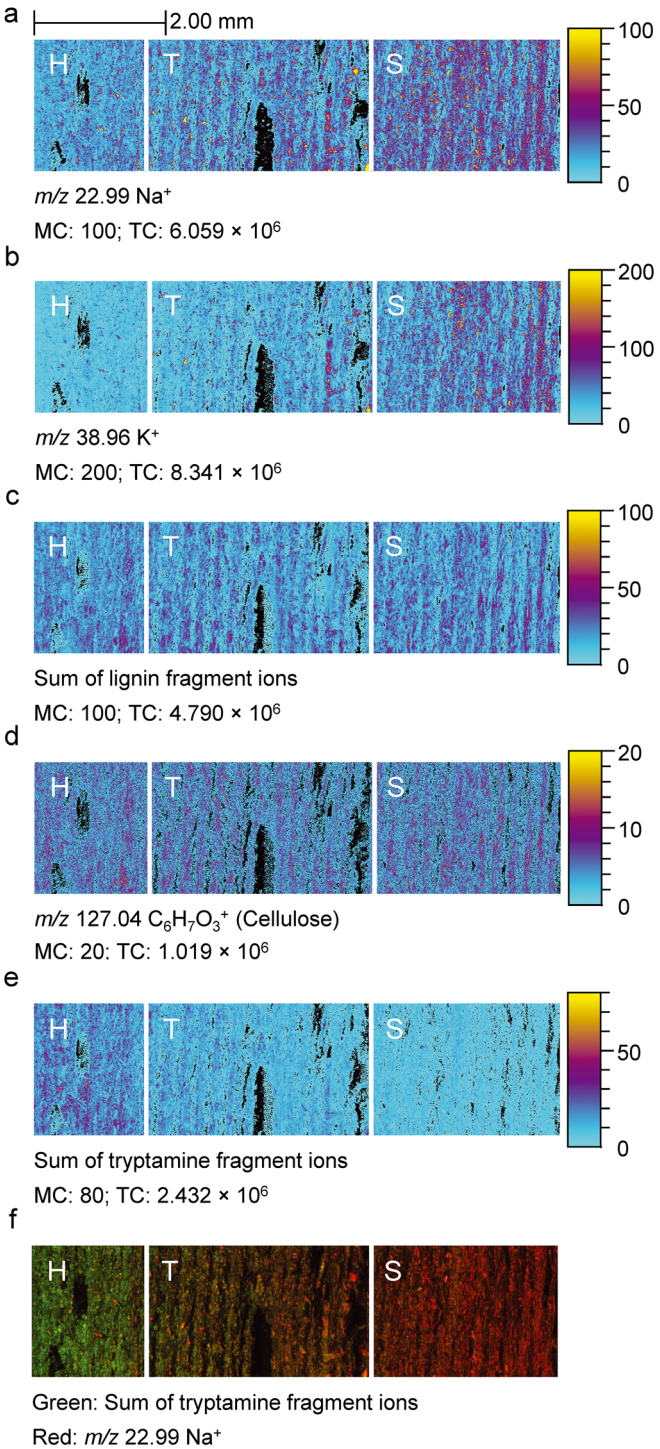

Figure 4. Ion images of a *D guianensis* radial section: (a) Na^+ at *m/z* 22.99; (b) K^+ at *m/z* 38.96; (c) sum of lignin fragment ions; (d) fragment ion of cellulose $[C_6H_7O_3]^+$, *m/z* 127.04; (e) sum of tryptamine fragment ions; (f) two color overlay between sodium (red) and the sum of tryptamine fragment ions (green). H, T and S indicate the heartwood, transition zone and sapwood, respectively.

Analysis of a radial section

The analysis of a radial section of *D. guianensis* allows detecting both inorganic ions and characteristic fragment ions of some structural polymers of wood, such as lignin and cellulose, as well as tryptamine characteristic fragment ions, in a single experiment. Figure 4(a) and Fig. 4(b) show the spatial distributions of sodium and potassium ions, respectively. These ions are mainly detected in the sapwood and the transition zone. Thanks to the attribution of ions published by Goacher *et al.* and Saito *et al.*, it is possible to find peaks in the spectra, which are characteristic of fragment ions of G-lignin ($C_8H_9O_2^+$ at *m/z* 137.06 and $C_8H_7O_3^+$ at *m/z* 151.05) and of S-lignin ($C_9H_{11}O_3^+$ at *m/z* 167.07 and $C_9H_9O_4^+$ at *m/z* 181.06).[13,30,31] Characteristic fragment ions of H-lignin were not detected. After checking the spatial correlation between all the detected lignin fragment ions, the corresponding ion images were summed. Figure 4(c) shows the spatial distribution of the sum of lignin fragment ions detected at the surface of the radial section. Lignin is homogenously distributed on all the wood parts. A cellulose fragment ion ($C_6H_7O_3^+$ at *m/z* 127.04) was also detected, and its spatial

Journal of MASS SPECTROMETRY

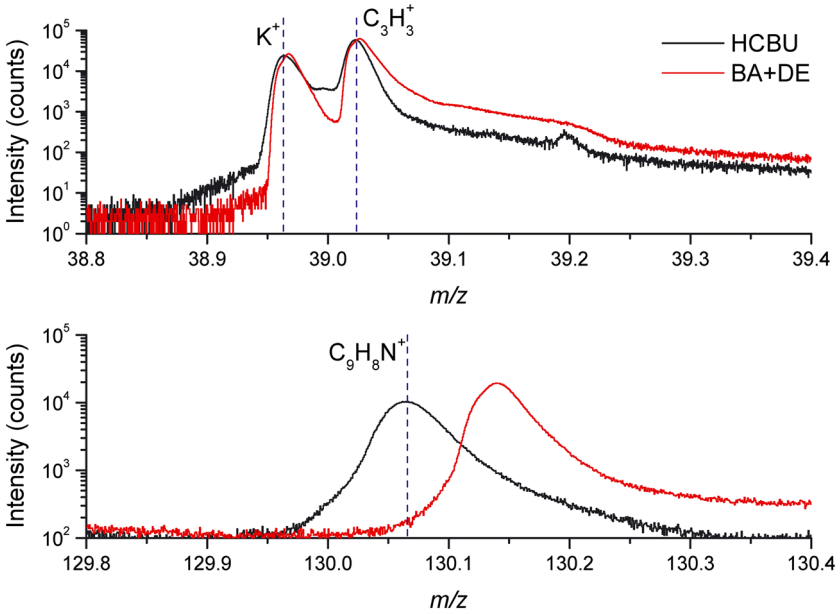

Figure 5. Overlay of two mass spectra recorded on a wood section surface in high current bunched mode (continuous extraction, black) and in BA + DE mode (delayed extraction, red). Both mass spectra have been calibrated using light mass ions between *m/z* 15 and 41. The dashed vertical lines indicate the exact mass of the labeled ions. BA, burst alignment; DE, delayed extraction.

distribution is shown in Fig. 4(d). This ion image indicates that cellulose signals are present at the same level in the different parts of the wood. These results show that the composition in structural polymers remain the same during the heartwood formation. In the total mass spectrum, ions at *m/z* 130.07 and *m/z* 144.08 have been detected. By comparison with the pure tryptamine mass spectrum shown in Fig. 1 (a), these ions have been assigned to the tryptamine fragment ions $C_9H_8N^+$ and $C_{10}H_{10}N^+$, respectively. Their signal is stronger in heartwood.

This analysis of a radial section of *D. guianensis* shows that sodium and potassium are less concentrated in the heartwood than in the sapwood. On the contrary, the amount of tryptamine has been found to increase from the sapwood to the heartwood. Inorganic compounds may be removed from the cells before senescence of the parenchyma cells, and raw sap circulating in xylem contains mostly water and salts. This phenomenon has already been described in the literature,[12,32] and it is known to allow some wood species to grow in poor soils.[33] However, these data were acquired at a moderate spatial resolution of 8 μm and cannot provide any information at the cellular scale, or tell precisely in which cells tryptamine is located. High spatial resolution experiments are thus mandatory.

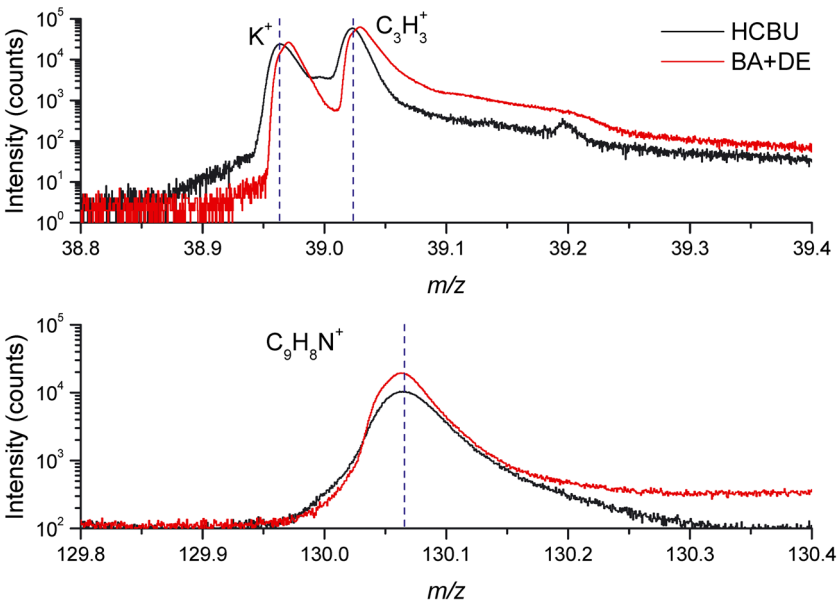

Figure 6. Overlay of two mass spectra recorded on a wood section surface in high current bunched (HCBU) mode (continuous extraction, black) and in BA + DE mode (delayed extraction, red). Mass calibration in HCBU mode was carried out with light mass ions and with heavier ions surrounding the peaks of interest for BA + DE mode. The dashed vertical lines indicate the exact mass of the labeled ions. BA, burst alignment; DE, delayed extraction.

Table 2. Mass resolution and mass accuracy measured at different mass-to-charge ratio in both HCBU and BA + DE modes

Formula	CH_3^+	CHO^+	$CaOH^+$	$C_9H_8N^+$	$C_9H_{11}O_3^+$
m/z	15.02	29.00	56.97	130.07	167.07
Mass resolution in HCBU mode (M/ΔM, FWHM)	2376	2925	3128	2766	2420
Mass accuracy in HCBU (ppm)	6	−5	−37	−15	−20
Mass resolution in BA + DE mode (M/ΔM, FWHM)	996	3374	4790	4470	4397
Mass accuracy in BA + DE (ppm)	620	29	−14	5	−50

BA, burst alignment; DE, delayed extraction; HCBU; high current bunched

High spatial resolution analysis of a transverse section

Mass calibration when using the DE

With a continuous extraction of secondary ions, a linear relationship between the time-of-flight and the root square of the mass-to-charge ratio is verified over the entire mass spectrum leading to an easy internal mass calibration using light mass fragment ions. When using the DE, an energy deficit of secondary ions is inversely correlated to their mass-to-charge ratio. The linearity between the time-of-flight and the root square of the mass-to-charge ratio is no longer valid over the entire mass spectrum. This is illustrated in Fig. 5, which shows an overlay of two spectra recorded on a wood section surface in HCBU mode (black line) and in BA + DE mode (red line). Both mass spectra were calibrated using CH_3^+, H_3O^+, $C_2H_3^+$ and $C_3H_5^+$ ions, at *m/z* 15.02, 29.02, 27.03 and 41.04, respectively. For the low mass ions such as K^+ and $C_3H_3^+$, this mass calibration ensures low deviations with the two modes. On the contrary for higher mass ions such as $C_9H_8N^+$ at *m/z* 130.07, a deviation of 0.1 Da is measured in the case of the BA + DE mode (DE) while the calibration leads to a good mass precision (<50 ppm) in the HCBU mode (continuous extraction). To obtain a better mass calibration, it is necessary to surround the mass range of interest by the peaks used to calibrate, similar to what is carried out in MALDI-TOF mass spectrometry in which a DE is also used. In the present study, the characteristic ions of the structural polymers of wood can be used.[13] Figure 5 and Fig. 6 show the mass spectra obtained in HCBU mode and calibrated using light mass ions, and the one obtained in BA + DE mode, calibrated using $C_7H_7^+$, $C_7H_9^+$, $C_7H_{11}^+$, $C_8H_9^+$ and $C_{11}H_9O_3^+$ ions at *m/z* 91.05, 93.07, 95.09, 105.07 and 189.06, respectively. It can be seen that the mass accuracy is improved in the latter case. Another way to improve mass accuracy when using DE could have been to make an external calibration, as shown recently by Shon *et al.*[34] However, such a procedure would have not been possible in the present case because of the very small size of the sample. This is therefore why an internal calibration has been preferred.

Table 2 lists the measurements of the mass resolution and mass accuracy for some ions. In the BA + DE mode, only CH_3^+ exhibits a significant mass shift.

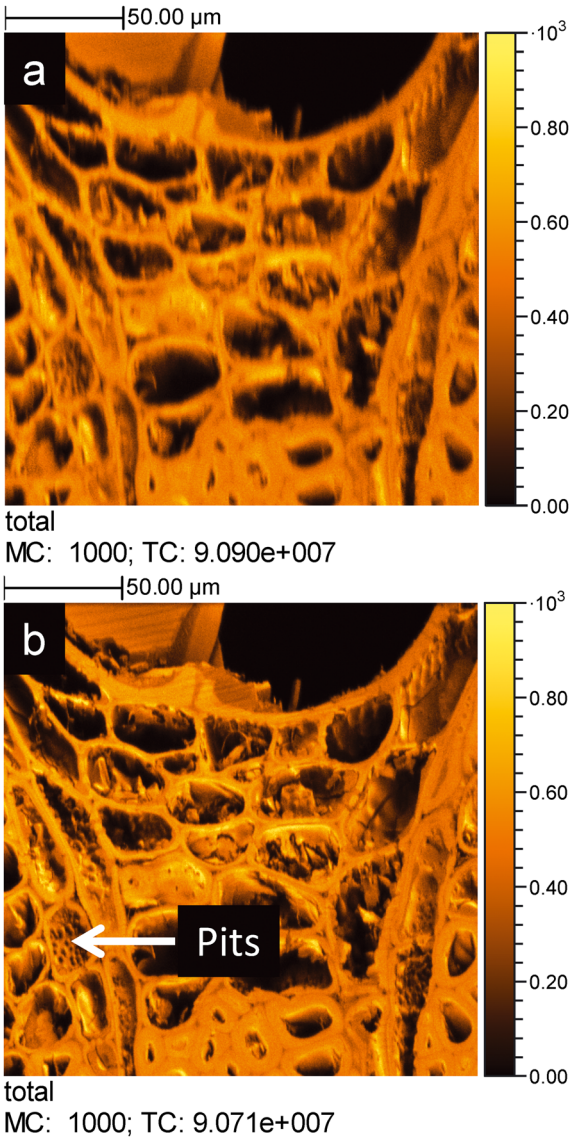

Figure 7. Total ion image of a *D. guianensis* transversal section (transition zone) without (a) and with (b) the use of lateral shift correction function in SURFACE LAB 6.5 software.

Improvement of ion image quality with automatic lateral shift correction

The SURFACE LAB 6.5 software provides a function, which allows compensating for some eventual shifts of the primary ion beam position during the acquisition. This function, called *lateral shift correction*, aligns the images between different scans. Figure 7 shows the same ion image without and with the use of the lateral shift correction algorithm. When the algorithm is applied, the resolution of the image is improved and some subcellular structures are observable. For example, the white arrow in Fig. 7(b) highlights the cell pits. These little structures are difficult to distinguish in the initial image.

Journal of MASS SPECTROMETRY

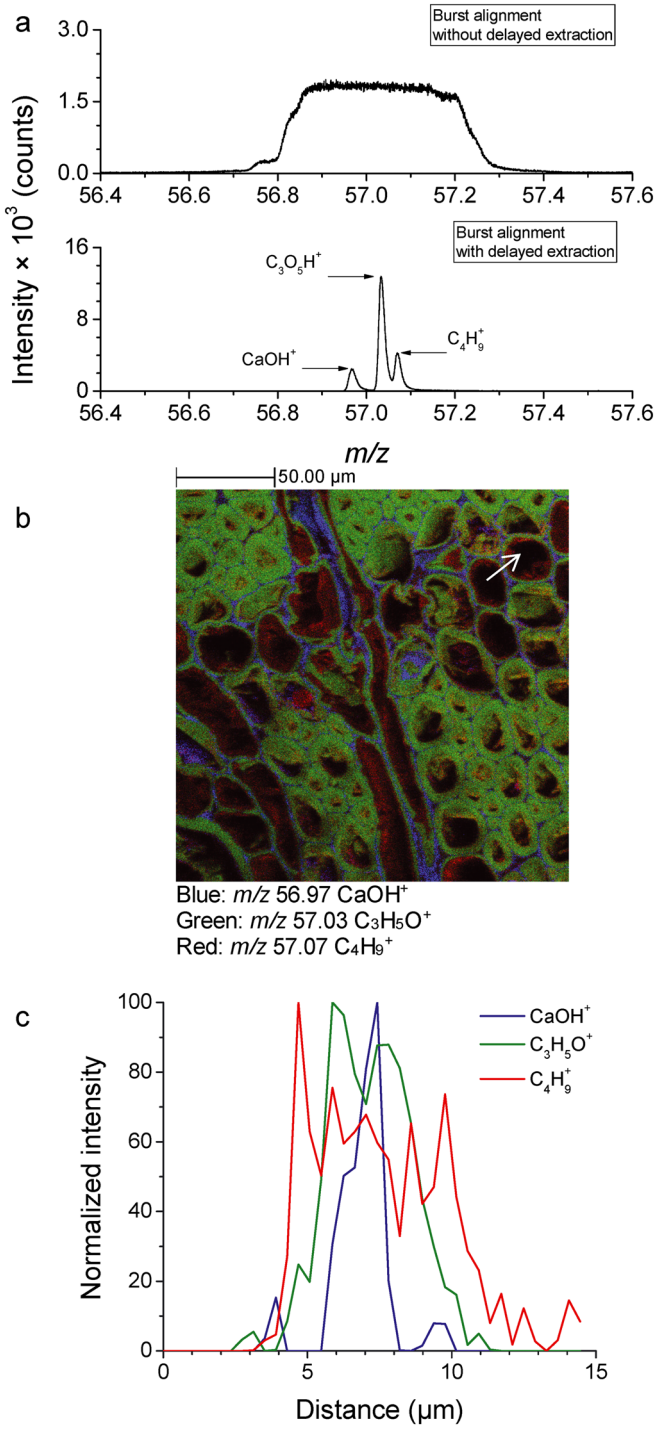

Figure 8. Interest of the delayed extraction. (a) Mass spectra recorded in the 56.4–57.6 *m/z* range from the same wood transversal section (heartwood), without (top) and with (bottom) the delayed extraction. (b) Three color overlay of three ion images: $CaOH^+$, *m/z* 56.97 (blue); $C_3H_5O^+$, *m/z* 57.03 (green); and $C_4H_9^+$, *m/z* 57.07 (red). The white arrow shows the line-scan along which the 3 ion intensities were extracted. (c) Line-scan of $CaOH^+$, $C_3H_5O^+$ and $C_4H_9^+$ ion intensities.

Comparison between acquisition with and without the delayed extraction

The same wood section was analyzed twice in the BA mode, without and with DE, respectively. Figure 8(a) shows parts of the two mass spectra recorded with the two modes, in a *m/z*

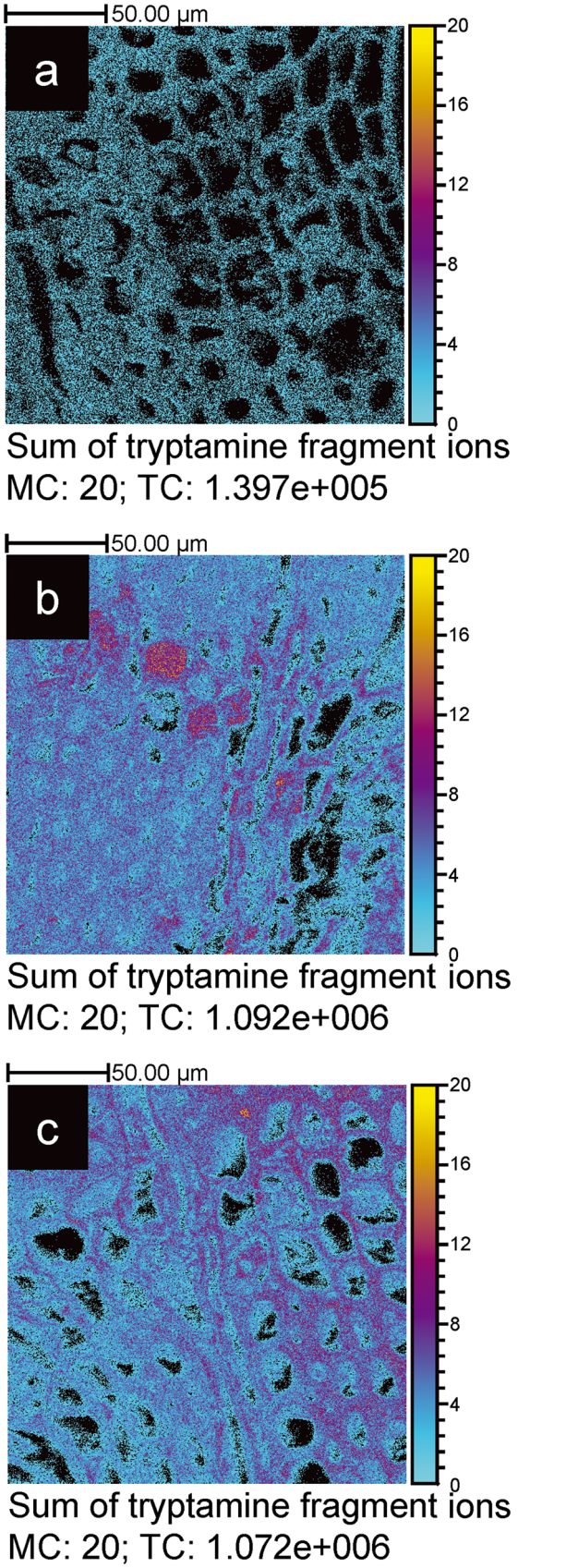

Figure 9. Ion images of the sum of tryptamine fragment ions recorded at the surface of sections of *D. guianensis* transversal sections in: (a) the sapwood; (b) the transition zone; and (c) the heartwood. Images have been cropped to zoom on areas of interest of 200 µm × 200 µm size.

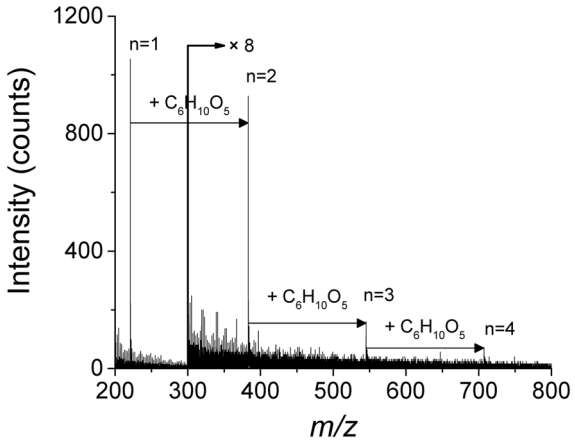

Figure 10. Part of negative ion mass spectrum extracted from the region of interest of small structures in the sapwood parenchyma cells.

scale from 56.4 to 57.6. It shows that the enhancement of mass resolution provided by the DE allows separating three quasi-isobaric ions, which were not distinguishable in the spectrum obtained without the DE. Figure 8(b) shows a three color overlay of the images of these three ions, which are assigned to $CaOH^+$ at *m/z* 56.97, $C_3H_5O^+$ at *m/z* 57.03 and $C_4H_9^+$ at *m/z* 57.07. These three ions have different spatial distributions, which cannot be distinguished without the DE. The white arrow in Fig. 8(b) shows the line chosen for the extraction of these three ion intensities (line-scan). Result is shown in Fig. 8(c). Calcium is only detected in the pectin-rich cell corners. Pectin may chelate calcium. This shows the great advantage of using the BA + DE mode in analyzing complex structured material, combining both high spatial and mass resolution.

Detection of tryptamine in subcellular structures

Clean surfaces obtained from sapwood, transition zone and heartwood were analyzed according to the previously described experimental procedures, that is, the so-called BA + DE mode, the software lateral shift correction and the precise mass calibration. Figure 9 shows the images of the sum of tryptamine fragment ions recorded in different areas. In sapwood [Fig. 9(a)], tryptamine is less abundant and becomes more abundant in the lumen of parenchyma cells in the transition

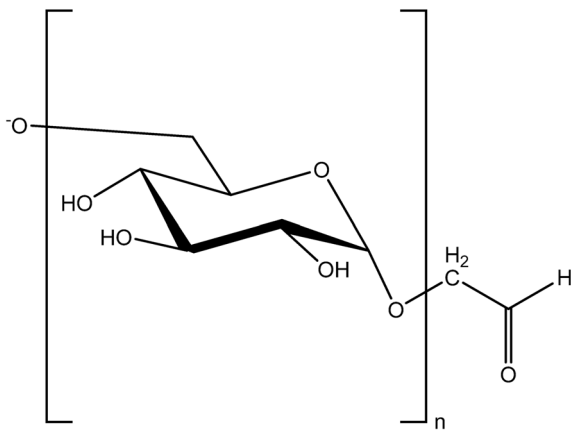

Figure 11. Structure of the detected negative ions, fragments of starch ions.

Table 3. Formulas, theoretical and measured mass of starch fragment ions and calculated standard deviation in parts-per-million

Number of units	Formula	Theoretical mass (*m/z*)	Measured mass (*m/z*)	Standard deviation (ppm)
1	$C_8H_{13}O_7^-$	221.066	221.071	22
2	$C_{14}H_{23}O_{12}^-$	383.119	383.126	18
3	$C_{20}H_{33}O_{17}^-$	545.172	545.169	−5
4	$C_{26}H_{43}O_{22}^-$	707.225	707.263	54

zone [Fig. 9(b)], before being diffused and detected in all the cell walls of the heartwood [Fig. 9(c)]. These three ion images show that tryptamine is produced by the parenchyma cells before their apoptosis. This indicates that this metabolite is involved in the heartwood formation of *D. guianensis*. It is produced in large amount by the senescent parenchyma cells and may trigger neighboring parenchyma cell apoptosis. Furthermore, this molecule is a toxic metabolite against the wood pests, and is a biosynthetic precursor of the other indole alkaloids described in this species.[21]

Detection of starch structures

Figure 10 shows the negative ion mass spectrum extracted from the region of interest (ROI) from small structures present in parenchyma cells in the sapwood. Peaks corresponding to already-described polysaccharide fragment ions[35] (Fig. 11) are intense in this ROI. Table 3 summarizes the theoretical and measured *m/z* and standard deviations for these polysaccharide fragment ions. In TOF-SIMS, it is difficult to distinguish starch from cellulose, because of their structural similarity. The difference between these two polymers is only in the orientation of the anomeric bond.

Figure 12 shows ion images of the sum of polysaccharide fragment ions, which can be assigned to cellulose or starch. These fragment ions are detected in all the cell walls but ion images clearly differentiated starch granules in parenchyma cells, with high local intensities of polysaccharide fragment ions. The signal detected in the cell walls is due to cellulose. As expected, we observe that wood cells consume all the available nutriments before their apoptosis for the biosynthesis of extractives. This also contributes to explain the natural durability of the heartwood of *D. guianensis*. The heartwood does not contain starch, and therefore is less nutritive for wood-boring insects and fungi, which need starch as a nutriment for their development and reproduction.[33,36]

Detection of silica ions

Silicon containing ions, which could be attributed to silica, were detected and used for the reconstruction of silica ions images. Silica grains presumably contribute to damage insect mandibles, as proposed by de Silva and Hillis.[37] Figure 13 shows the spatial distribution of the sum of these silica ions, which have been detected in all the wood parts. Figure 14 shows the negative ion mass spectrum extracted from the ROI of a silica grain. Table 4 summarizes the formula of the detected silica ions, their theoretical masses and their measured masses and standard deviations.

Conclusion

Dense tropical woods are complex material difficult to cut for obtaining a plane surface. Different sample preparation methods

Journal of MASS SPECTROMETRY

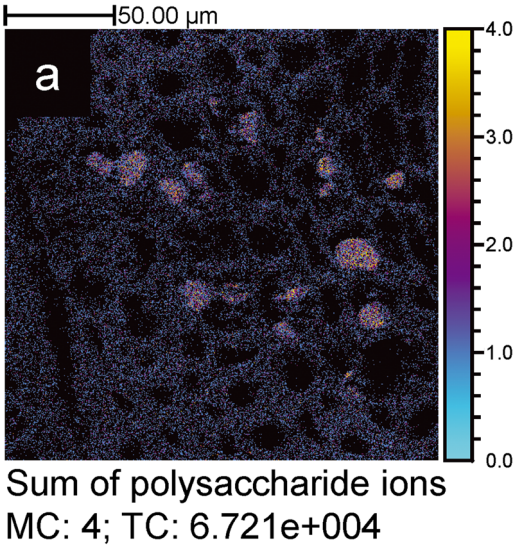

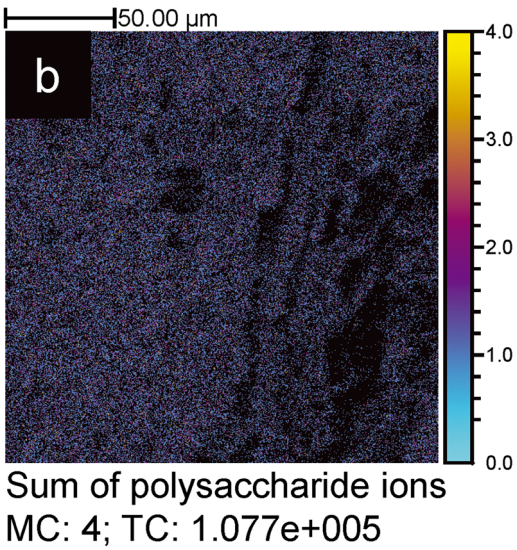

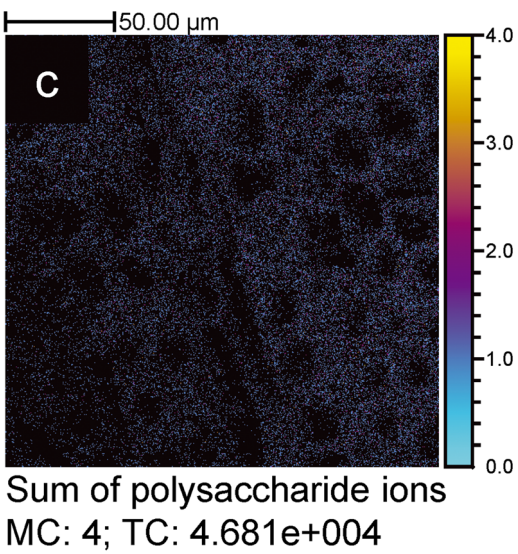

Figure 12. Ion images of the sum of polysaccharide fragment ions recorded at the surface of sections of *D. guianensis* transversal sections in: (a) the sapwood; (b) the transition zone; and (c) the heartwood. Images have been cropped to zoom on areas of interest of 200 µm × 200 µm size.

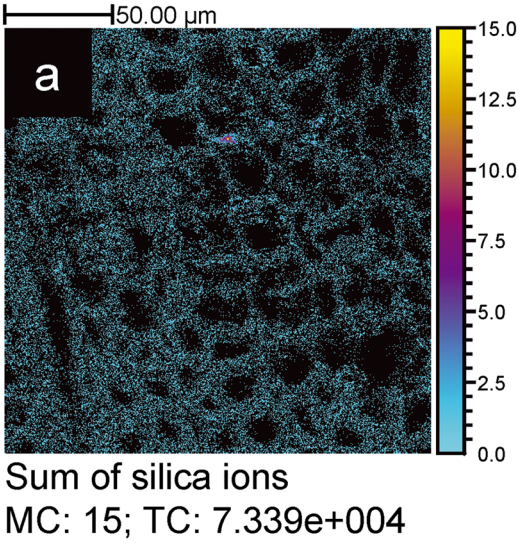

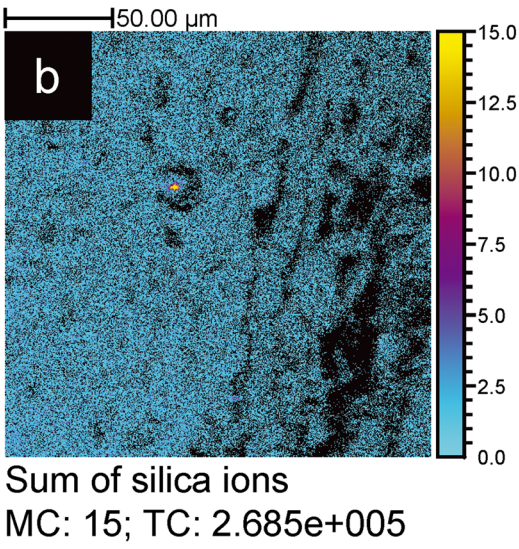

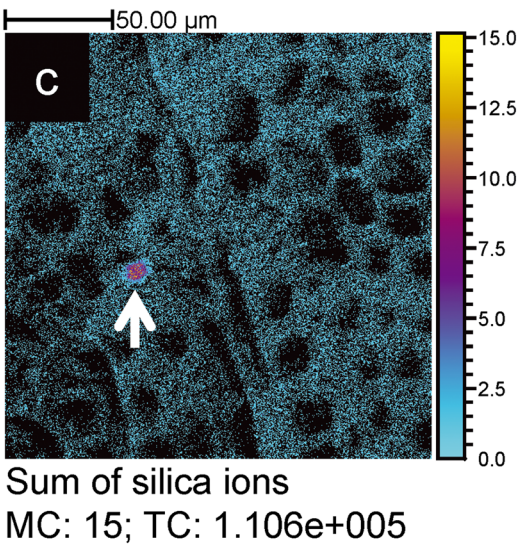

Figure 13. Ion images of the sum of silica ions recorded at the surface of sections of *D. guianensis* transversal sections in: (a) the sapwood; (b) the transition zone; and (c) the heartwood. Images have been cropped to zoom on areas of interest of 200 µm × 200 µm size. The white arrows show the silica grains.

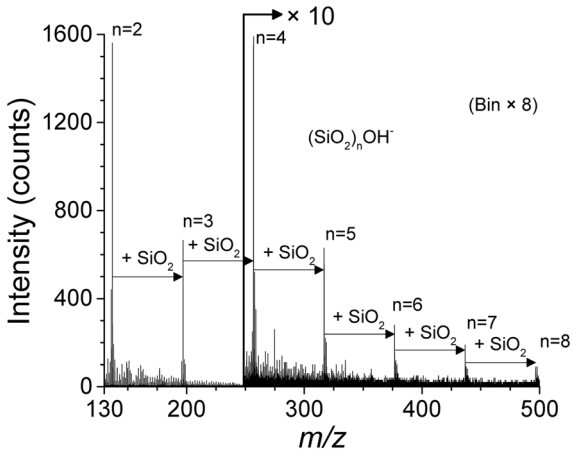

Figure 14. Part of negative ion mass spectrum extracted from the region of interest of a silica grain.

Table 4. Formulas, theoretical and measured mass of silica ions and calculated standard deviation in parts-per-million

Formula	Theoretical mass (*m/z*)	Measured mass (*m/z*)	Standard deviation (ppm)
SiO_3^-	75.9617	75.9635	23.70
$SiHO_3^-$	76.9695	76.971	19.49
$Si_2HO_5^-$	136.9363	136.9433	51.12
$Si_3HO_7^-$	196.9030	196.9104	37.58
$Si_4HO_9^-$	256.8698	256.8847	58.00
$Si_5HO_{11}^-$	316.8365	316.8563	62.49

have been compared, and it has been found that the best way to obtain a flat surface while preserving the localization of the secondary metabolites is to trim sections using an ultramicrotome equipped with a diamond blade.

The delayed extraction of secondary ions was used to acquire ion images with both high spatial and mass resolutions. A careful mass calibration was made by using ion peaks that surround those of interest. This requires knowing beforehand the chemical composition of the sample, at least partially.

Thanks to these appropriate sample preparation and delayed extraction, it was possible to study the spatial distribution of organics and inorganics in *D. guianensis* transverse sections, in sapwood, transition zone and heartwood, for a better understanding of heartwood formation. Three defense modes, which can be linked to the natural durability of *D. guianensis* heartwood, have been simultaneously illustrated by the TOF-SIMS analyses. A depletion of the starch used as nutrient by wood pests has been observed. Toxic metabolite tryptamine has been detected in the axial parenchyma cells in the transition zone, and in all the cell walls of the heartwood. Finally, silica grains have been detected in all the wood, from the sapwood to the heartwood.

Acknowledgements

Q. P. V. is indebted to the « Fondation pour le développement de la chimie des substances naturelles et ses applications » for a PhD research fellowship. We acknowledge the sponsorship from Chinese Scholarship Council (CSC) for T. F. PhD study (No. 201406310013). This work has benefited from an 'Investissement d'Avenir' grant managed by Agence Nationale de la Recherche (CEBA, ref. ANR-10-LABX-25-01). This work has benefited from the facilities and expertise of the Electron Microscopy facilities of Imagerie-Gif (http://www.i2bc.paris-saclay.fr/spip.php?article282). Julien Ruelle (INRA, UMR 1092 Laboratoire d'étude des ressources Forêt Bois, Centre INRA de Nancy-Lorraine 54280 Champenoux, France) is gratefully acknowledged for fruitful discussions.

References

[1] D. Touboul, A. Brunelle, O. Laprévote. Mass spectrometry imaging: towards a lipid microscope? *Biochimie* **2011**, *93*, 113–119.
[2] J. S. Fletcher, J. C. Vickerman. Secondary ion mass spectrometry: characterizing complex samples in two and three dimensions. *Anal. Chem.* **2013**, *85*, 610–639.
[3] L. Houssiau, M. Felicissimo, C. Bittencourt, J. J. Pireaux. ToF-SIMS applied to probe bixin in *Bixa orellana* seeds. *Appl. Surf. Sci.* **2004**, *231–232*, 416–419.
[4] C. Bittencourt, M. P. Felicissimo, J. J. Pireaux, L. Houssiau. ToF-SIMS characterisation of thermal modifications of bixin from *Bixa orellana* fruit. *J. Agric. Food Chem.* **2005**, *53*, 6195–6200.
[5] A. Seyer, J. Einhorn, A. Brunelle, O. Laprévote. Localization of flavonoids in seeds by cluster time-of-flight secondary ion mass spectrometry imaging. *Anal. Chem.* **2010**, *82*, 2326–2333.
[6] M. C. Perkins, G. Bell, D. Briggs, M. C. Davies, A. Friedman, C. A. Hart, C. J. Roberts, F. J. M. Rutten. The application of ToF-SIMS to the analysis of herbicide formulation penetration into and through leaf cuticles. *Colloids Surf. B.* **2008**, *67*, 1–13.
[7] T. Leefmann, C. Heim, A. Kryvenda, S. Siljeström, P. Sjövall, V. Thiel. Biomarker imaging of single diatom cells in a microbial mat using time-of-flight secondary ion mass spectrometry (ToF-SIMS). *Org. Geochem.* **2013**, *57*, 23–33.
[8] X. Li, K. Schirmer, L. Bernard, L. Sigg, S. Pillai, R. Behra. Silver nanoparticle toxicity and association with the alga Euglena gracilis. *Environ. Sci.: Nano.* **2015**, *2*, 594–602.
[9] T. Imai, K. Tanabe, T. Kato, K. Fukushima. Localization of ferruginol, a diterpene phenol, in Cryptomeria japonica heartwood by time-of-flight secondary ion mass spectrometry. *Planta* **2005**, *211*, 549–556.
[10] E. N. Tokareva, P. Fardim, A. V. Pranovich, H. P. Fagerholm, G. Daniel, B. Holmbom. Imaging of wood tissue by ToF-SIMS: critical evaluation and development of sample preparation techniques. *Appl. Surf. Sci.* **2007**, *253*, 7569–7577.
[11] K. Saito, T. Mitsutani, T. Imai, Y. Matsushita, K. Fukushima. Discriminating the indistinguishable sapwood from heartwood in discolored ancient wood by direct molecular mapping of specific extractives using time-of-flight secondary ion mass spectrometry. *Anal. Chem.* **2008**, *80*, 1552–1557.
[12] K. Saito, T. Mitsutani, T. Imai, Y. Matsushita, A. Yamamoto, K. Fukushima. Chemical differences between sapwood and heartwood of *Chamaecyparis obtuse* detected by ToF-SIMS. *Appl. Surf. Sci.* **2008**, *255*, 1088–1091.
[13] R. E. Goacher, D. Jeremic, E. R. Master. Expanding the library of secondary ions that distinguish lignin and polysaccharides in time-of-flight secondary ion mass spectrometry analysis of wood. *Anal. Chem.* **2011**, *83*, 804–812.
[14] C. Zhou, Q. Li, V. L. Chiang, L. A. Lucia, D. P. Griffis. Chemical and spatial differentition of syringyl and guaiacyl lignins in poplar wood via time-of-flight secondary ion mass spectrometry. *Anal. Chem.* **2011**, *83*, 7020–7026.
[15] S. Jung, M. Foston, U. C. Kalluri, G. A. Tuskan, A. J. Ragauskas. 3D chemical image using TOF-SIMS revealing the biopolymer component spatial and lateral distributions in biomass. *Angew. Chem. Int. Ed.* **2012**, *51*, 12005–12008.
[16] K. Saito, Y. Watanabe, M. Shirakawa, Y. Matsushita, T. Imai, K. Koike, Y. Sano, R. Funada, K. Fukazawa, K. Fukushima. Direct mapping of morphological distribution of syringyl and guaiacyl lignin in the xylem of maple by time-of-flight secondary ion mass spectrometry. *Plant J.* **2012**, *69*, 542–552.
[17] K. Kuroda, T. Fujiwara, T. Imai, R. Takama, K. Saito, Y. Matsushita, K. Fukushima. The cryo-TOF-SIMS/SEM system for the analysis of the chemical distribution in the freeze-fixed *Cryptomeria japonica* wood. *Surf. Interface Anal.* **2013**, *45*, 215–219.

[18] K. Saito, Y. Watanabe, Y. Matsushita, T. Imai, T. Koike, Y. Sano, R. Funada, K. Fukazawa, K. Fukushima. Aluminum localization in the cell walls of the mature xylem of maple tree detected by elemental imaging using time-of-flight secondary ion mass spectrometry (TOF-SIMS). *Holzforschung* **2014**, *68*, 85–92.
[19] L. Gerber, V. M. Hoang, L. Tran, H. A. T. Kiet, P. Malmberg, J. Hanrieder, A. Ewing. Using imaging ToF-SIMS data to determine the cell wall thickness of fibers in wood. *Surf. Interface Anal.* **2014**, *46*, 225–228.
[20] M. Bereau, T. S. Barigah, E. Louisanna, J. Garbaye. Effects of endomycorrhizal development and light regimes on the growth of *Dicorynia guianensis* Amshoff seedlings. *Ann. For. Sci.* **2000**, *57*, 725–733.
[21] J. B. S. Anouhe, A. A. Adima, F. B. Niamké, D. Stien, B. K. Amian, P. A. Blandinières, D. Virieux, J. L. Pirat, S. Kati-Coulibaly, N. Amusant. Dicorynamine and harmalan-*N*-oxide, the new ß-carboline alkaloids from *Dicorynia guianensis* Amsh. heartwood. *Phytochem. Lett.* **2015**, *12*, 158–163.
[22] Q. P. Vanbellingen, N. Elie, M. J. Eller, S. Della-Negra, D. Touboul, A. Brunelle. Time-of-flight secondary ion mass spectrometry imaging of biological samples with delayed extraction for high mass and high spatial resolutions. *Rapid Commun. Mass Spectrom.* **2015**, *29*, 1187–1195.
[23] E. Rutishauser, D. Barthélémy, L. Blanc, N. Eric-André. Crown fragmentation assessment in tropical trees: method, insights and perspectives. *For. Ecol. Manage.* **2011**, *461*, 400–407.
[24] R. N. S. Sodhi. Time-of-flight secondary ion mass spectrometry (TOF-SIMS): versatility in chemical and imaging surface analysis. *Analyst* **2004**, *129*, 483–487.
[25] D. Touboul, F. Kollmer, E. Niehuis, A. Brunelle, O. Laprévote. Improvement of biological TOF-SIMS imaging with a bismuth cluster ion source. *J. Am. Soc. Mass Spectrom.* **2005**, *16*, 1608–1618.
[26] A. Brunelle, D. Touboul, O. Laprévote. Biological tissue imaging with time-of-flight secondary ion mass spectrometry and cluster ion sources. *J. Mass Spectrom.* **2005**, *40*, 985–999.
[27] W. Sandermann, W. Lange. Studien über Wasserbauhölzer-I. Mitteilung. Chemische Untersuchung des Holzes von Angélique (Basralocus-*Dicorynia guianensis* Amsh.) (Studies on wood used for underwater construction. I. Chemical investigation on angelique wood (*Dicorynia guianensis*). *Holzforschung* **1967**, *21*, 154–157.
[28] V. Mazel, P. Richardin, D. Touboul, A. Brunelle, P. Walter, O. Laprévote. Chemical imaging techniques for the analysis of complex mixtures: New application to the characterization of ritual matters on African wooden statuettes. *Anal. Chim. Acta* **2006**, *570*, 34–40.
[29] P. Richardin, V. Mazel, P. Walter, O. Laprévote, A. Brunelle. Identification of different copper green pigments in renaissance paintings by cluster-TOF-SIMS imaging analysis. *J. Am. Soc. Mass Spectrom.* **2011**, *22*, 1729–1736.
[30] K. Saito, T. Kato, Y. Tsuji, K. Fukushima. Identifying the characteristic secondary ions of lignin polymer using ToF-SIMS. *Biomacromolecules* **2005**, *6*, 678–683.
[31] K. Saito, T. Kato, H. Takamori, T. Kishimoto, K. Fukushima. A New analysis of the depolymerized fragments of lignin polymer using ToF-SIMS. *Biomacromolecules* **2005**, *6*, 2688–2696.
[32] P. Meerts. Mineral nutrient concentrations in sapwood and heartwood: a literature review. *Ann. For. Sci.* **2002**, *59*, 713–722.
[33] A. M. Taylor, B. L. Gartner, J. J. Morrell. Heartwood formation and natural durability – a review. *Wood Fiber Sci.* **2002**, *34*, 587–611.
[34] H. K. Shon, S. Yoon, J. H. Moon, T. G. Lee. Improved mass resolution and mass accuracy in TOF-SIMS spectra and images using argon gas cluster ion beams. *Biointerphases* **2016**, *11*, 02A321.
[35] P. M. Baldwin, C. D. Melia, M. C. Davies. The surface chemistry of starch granules studied by time-of-flight secondary ion mass spectrometry. *J. Cereal Sci.* **1997**, *26*, 329–346.
[36] B. C. Peters, J. W. Creffield, R. H. Eldridge. Lyctine (coleoptera: brostrichidae) pest of timber in Australia: a literature review and susceptibility testing protocol. *Aust. For.* **2002**, *65*, 107–119.
[37] D. de Silva, W. E. Hillis. The contribution of silica to the resistance of wood to marine borers. *Holzforschung* **1980**, *34*, 95–97.